ORIGINAL PAPER

INVESTIGATION OF Ni-Cu THIN FILMS MAGNETIC SENSORS DEPOSITED ON SiO_2 SUBSTRATES BY SPUTTERING

COSMIN COBIANU[1], MIHAIL FLORIN STAN[1], IULIAN BANCUTA[1*], NICOLAE FIDEL[1]

Manuscript received: 23.09.2019; Accepted paper: 04.11.2019; Published online: 30.12.2019.

Abstract. *The objective of this paper it is to produce magnetic sensors with thin Ni-Cu layers with GMR, sputtered on SiO_2 substrate, which could be used as magnetic field sensors. Determination of the thickness and uniformity of the magnetic sensor layers it is done by optical microscopy and atomic force microscopy (AFM) for different areas. Finally, measurements were made using the MF100 AC/DC magnetometer and the experimental results were processed. As a magnetic field source, we used a ferrite ring magnet, Y35, with 6 kg force (about 58.8 N).*

Keywords: *magnetic sensors with GMR, sputtering, thin layers, AFM, MF100 AC/DC, magnetometer.*

1. INTRODUCTION

Magnetic sensors have a broad range of applications such as measurement magnetic field, read-aut of magnetic memories, non-contact switching, traffic control, mineral prospecting purposes, in biomedical applications such as brain function mapping and magnetic imaging [1-3].

Magnetic sensors used in nearly all engineering and industrial sectors, such as high-density magneting recording, navigation, target detection and tracking, antitheft systems, geomagnetic measurement, nondestructive testing, magnetic marking and labeling, space research, and biomagnetic measurements in the human body [1, 4-6].

Magnetoresistive (MR) sensors are showing a change in their rezistance with an external magnetic field. GMI effect is described as large changes happening in the AC impedance in a ferromagnetic material running with small AC current under the effect of magnetic field. The GMI sensors exhibit many advantages over the conventional types of sensors [1, 7, 8].

The Magnetoimpedance (MI) structures can be deposited onto glass substrates at room temperature by RF sputtering in Ar atmosphere (Pressure it is $3x10^{-7}$ mbar, the value of the argon pressure it is $3.8x10^{-3}$ mbar). The MI ratios for the total impedance $\Delta Z/Z$ and its real part $\Delta R/R$ were calculated with respect to their values at field of magnetic saturation H_{max} = 115Oe. MI it is definite as follows: $\Delta Z/Z = 100 \times [Z(H) - Z(H_{max})] / Z(H_{max})$ for total impedance and $\Delta R/R = 100 \times [R(H) - R(H_{max})] / R(H_{max})$ for real part of the impedance. The MI sensitivity it is defined as $(\Delta Z/Z) = (\Delta Z/Z) / \Delta H$ or s $(\Delta R/R) = (\Delta R/R) / DH$, where ΔH = 0.1 Oe – increment for a magnetic field. The maximum values of the MI ratio and MI

[1] Valahia University of Targoviste, Faculty of Electrical Engineering, Electronics and Information Technology, 130004 Targoviste, Romania. E-mails: cosmincobianu@yahoo.com; flo.stan@gmail.com; nicolae.fidel@valahia.ro. **Corresponding Author :* iulian_bancuta@yahoo.com;

sensitivity for total impedance were denoted as $(\Delta Z/Z)_{max}$ and s $(\Delta Z/Z)_{max}$ and corresponding them frequencies f $[(\Delta Z/Z)_{max}]$ and f [s $(\Delta Z/Z)_{max}$]. The maximum value of the MI ratio and MI sensitivity for the real part of the total impedance were denoted as $(\Delta R/R)_{max}$ and s $(\Delta R/R)_{max}$ and corresponding frequencies as f $[(\Delta R/R)_{max}]$ and f [s $(\Delta R/R)_{max}$] [9-11].

2. INSTALLATION USED FOR METAL AND DIELECTRIC LAYERS DEPOSITION BY SPUTTERING

The equipment used for obtaining thin films by physical deposition method from vapour state (PVD) is INTERCOVAMEX H2 thermal evaporator. The INTERCOVAMEX H2 is a thermal evaporator configured for evaporation of Al thin films onto silicon and glass/quartz substrates. This equipment belongs to the the Institute of Multidisciplinary Research for Science and Technology from Valahia University of Targoviste, with the acronym ICSTM-UVT [12]. The device contains two sources of spraying or magnetrons, which can be loaded with the desired coating composition material. The sputtering depositon is carried out with high-voltage DC or RF argon plasma. Up to 6 sequential materials can be deposited on substrates up to 250 mm in diameter. The equipment consists of: stainless steel chamber of 454 mm height x 454 mm width x 454 mm length, working mode is in high vacuum (< $5x10^{-8}$ torr). The system includes: DC or RF high-voltage argon plasma, rotating the substrate support with 4" scale, support for heater substrates up to 350^{o}C, a system for measuring the thickness of the deposited layer using quartz crystal microbalance, gas delivery system (Ar, N2 and compressed air) and evacuation system.

Figure 1. INTERCOVAMEX H2 sputtering.

To achieve the thin Ni-Cu layers, metal targets of very high purity (Cu target - 99.99% and Ni target - 99.995%) were used, and during deposition the substrate it is rotated with 30

rpm and heated slightly to a temperature of 40 °C. The argon flux (99.996% purity) at wich the deposition it is made is relatively low between 14 and 25 sccm, and the generator power is in the upper range of 750 W. The deposition of Ni-Cu thin films it is performed in high vacuum (15x10-6 torr) [12].

3. DIFFERENT CONFIGURATIONS OF MULTILAYERS MAGNETIC SENSORS

In a first phase of the research, the authors were concerned with the comparative analysis and analysis of Magnetic Sensors with thin Cu-Co layers deposited on SiO_2 and Sital substrates with GMR (giant magnetoresistance) [13, 14]. These sensors were deposited with the PLD (Pulsed Laser Deposition) method. Further, the research focused on depositing by GMR sputtering of Ni-Cu magnetic sensors on different types of supports. This paper presents the results obtained for SiO_2 support deposits.

Hereinafter are various structures that have been previously developed by various research teams.

Although certain theoretical estimations were developed about over fifteen years ago up to now there were no systematic experimental studies of the influence of the thickness of the conductive lead on MI [10, 15, 16]. In [9] authors studied the magnetic properties and MI for [FeNi(100 nm) / Cu(3.2 nm)]$_4$/ FeNi(100 nm)/Cu(L_{Cu})/ [FeNi(100 nm) / Cu(3.2 nm)]$_4$/ FeNi(100 nm) multilayers deposited in the shape of the stripes with variable thickness (LCu) of the Cu lead. The thickness of Cu is in a range of 3.2 to 1000 nm. All the prepared MI multilayers have the previous structure.

In paper [18] authors studied two Pt47/(Cox/Pt41)$_2$/ Cox/Pt22A multilayers with x = 3A and 5A were deposited on (100) Si/SiO_2 substrates using DC magnetron sputtering. The PMA in the multilayers it is confirmed by polar magneto-optical Kerr effect (MOKE) measurements. The multilayers were then patterned into 10-mm-wide Hall structures. Prior to the irradiation, an 8 nm SiO_2 layer it is deposited on the top for protection. Ga ion FIB irradiation it is performed on the devices with a commercial FIB (FEI Strata 201). The incident energy of the Ga ions it is 30 keV, and a 1.5 pA current it is used to dose the required area of the devices. The beam diameter is about 10 nm and the distance between neighboring pixels is 7.5 nm.

A series of stripe-shaped samples 2 mm long and from 50 to 130 mm wide were patterned using photolithographic methods [18]. The samples consist of multilayered sandwich (MS) structures [Py(170 nm) / Ti(6nm)]$_3$ / Cu(250nm)/ [Ti(6nm) / Py(170 nm)]$_3$, deposited by DC sputtering onto Si(100) wafers topped with SiO_2 (400nm). A well-defined transverse magnetic anisotropy with the anisotropy field Hk ≈ 320 A/m it is induced during the deposition process by the application of an in-plane constant magnetic field of 20 kA/m.

4. EXPERIMENTAL PROCEDURE

A total of 26 square and circular shaped sensors were made simultaneously by DC sputtering and the results presented in the paper are those of a sensor in the center of the support layer, 5 mm in diameter and with the sandwich structure (7 layers): SiO_2(1mm)/Cu(5μm)/Ni(12nm)/Cu(15nm)/....Ni(12nm)/Cu(100nm); a sensor for which the measurements indicated the best characteristics.

To obtain these sensors, we started from a glass substrate of 1mm thick over which a continuous and uniform copper layer of 5 μm it is applied by sputtering, which will be used as the lower contact of the sensors made. Over this layer a mask of vinyl chloride - C_2H_3Cl (PVC) of 100μm thick it is made, mask that will serve to form the shape of the sensors (circular or square) and at the same time to achieve the other 5 successive thin layers. The thin layers were also made by Ni and Cu sputtering, each layer having a thickness of between 10 and 15nm, a thickness measured during deposition with a quartz crystal microbalance (QCM) inside the sputtering. The 7th layer deposited it is from Cu representing the upper layer and having a thickness of 100nm (Figures 2, 3, 4 and 5). On this layer, the conductor weld will be made with the silver paste. Using the Ntegra Prima atomic microscope and the optical microscopy (PriomoStar microscope) at Valahia University from Târgoviște - the Institute of Multidisciplinary Research for Science and Technology, it is possible to check the thickness of the deposited layers as well as the uniformity of these layers (Figs. 8-13).

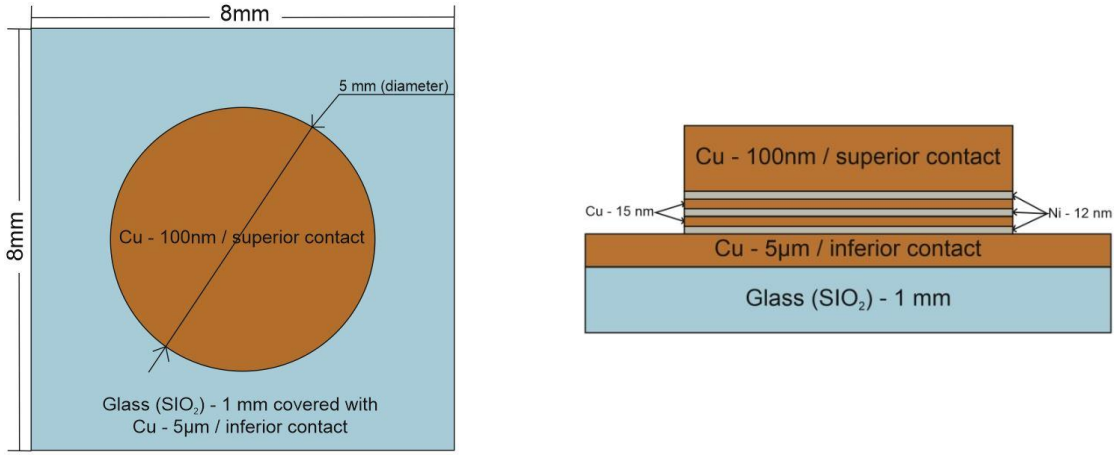

a) **b)**

Figure 2. Deposition scheme.

a) **b)**

Figure 3. One of the 26 sensors made, with its related contacts.

Using the relationships in [9-11], the GMR ratio for the Ni-Cu sensor, which is placed in the center of the magnet Y35, is calculated according to the magnetic field intensity and is defined by:

$$MR\ (H) = [R(H) - R(sat)] / R(sat) \quad (1)$$

$$MR\ (H) = (3.59 - 0.42) / 0.42 = 7.54\ \% \quad (2)$$

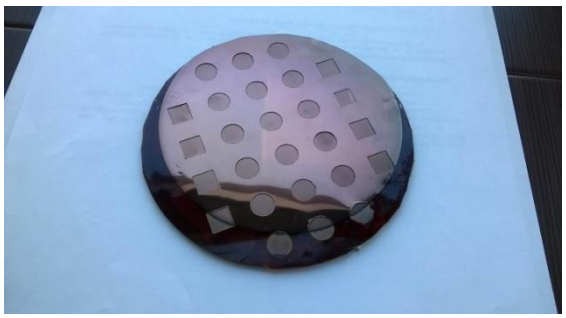

Figure 4. Overview masks plate - Ni/Cu sensors.

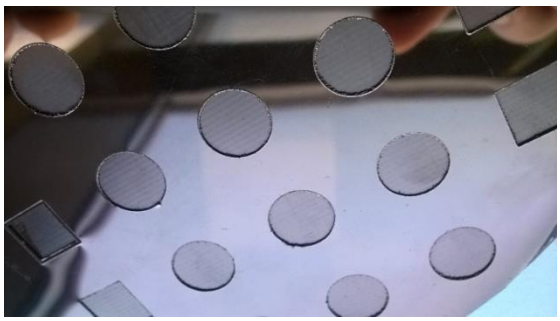

Figure 5. Picture detail masks plate - Ni/Cu sensors.

It is used as the magnetic field source, a ferrite ring magnet, Y35, having a force of 6 kg (about 58.8 N).

Figure 6. Y35 ring ferrite magnet.

Features of the Y35 ring ferrite magnet are: the magnet poles are on the flat faces; very good resistance to demagnetization; it does not need a protective layer. Ferrite magnets are made of ceramic material and therefore have dielectric properties. They are used in the most diverse areas such as: magnetic field source, magnetic separators, wind turbines, continuous current motors, sensors, medical equipment, experiments, etc.

The test stand is composed of a magnetometer MF100 AC/DC Magnetic Field Meter, a magnet that is used as a magnetic field source (a Y35 ring ferrite magnet), a tripod support on which the sensor is placed and the ruler that is used to measure the distance between the sensor and the source magnet. This distance ranged from 0.1 cm to 10 cm from cm in cm and the sensor it is placed both in the center and end of the Y35 source magnet.

Figure 7. Test stand.

The magnetic field meter (MF100) is an AC / DC meter equipped with a uniaxial magnetic sensor with Hall Effect and ATC (automatic temperature compensation), a polarity indicator (pole N / S), capable of storing certain values (Min / Max) and a protective cap.

5. ATOMIC AND MAGNETIC FORCE MICROSCOPY AFM

Atomic and magnetic force microscopy AFM were used in tapping mode for analyzing the morphology and the magnetic domains of the multilayers.

The atomic force microscope (Ntegra Prima by NT-MDT) is the device that allows the surface analysis of different types of samples with high accuracy and resolution. These measurements can be carried out in air, in liquid environment and at temperatures that can be controlled using integrated software and related equipment, specially adapted for this type of microscope. The experiments using this device can be carried out in three different modes (contact, semicontact and non-contact), the electronics being able to carry out operations in high frequency modes (up to 5 MHz). The images of the surfaces (insulating or conductive) obtained can be three dimensional having nano resolution in the lateral plane and under angstrom in the vertical plane. Atomic force microscopy is the most commonly used surface scanning technique (SPM). NTEGRA Prima has implemented several types of scanning: sample scanning, probe scanning and dual scanning. Because of this, the system is ideal for investigating with very high resolution (atomic or molecular level) of small samples, but also large samples and scanning intervals up to 100 μm x 100 μm x 10 μm can be investigated. The incorporation of three-axis closed-loop control sensors enables true scan detection, compensating for the inevitable imperfections of piezoceramics, such as nonlinearity, creep and hysteresis. NT-MDTs use sensors with the lowest noise level, which allows closed-loop controls on very small fields (up to 10 nm x 10 nm). Real-time scanning is possible thanks to the built-in NTEGRA Prima optical system, with a resolution of 1 μm [12].

The surface of the Ni-Cu layers has been measured with an Atomic Force Microscope (AFM) scanning a square of 10 μm x 10 μm, showing a homogeneous deposition of the layers inside the sensor. In the first 3 figures below (Figs. 8-10) are shown the 2D Scanning Capacitance Microscopy of the AFM in different areas, namely on the inside, on the outside and respectively on the line for a surface of 10x10 micrometres, showing a deposition homogeneous layers on the inside of the sensor. The following 3 figures (Figs. 11-13) are representations of AFM 3D Scanning Capacitance Microscopy images for the same areas as 2D images and for the same size.

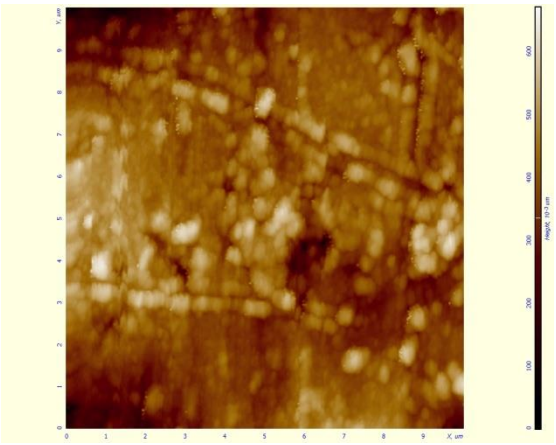

Figure 8. 2D SCM picture (10 x 10μm) on the outside

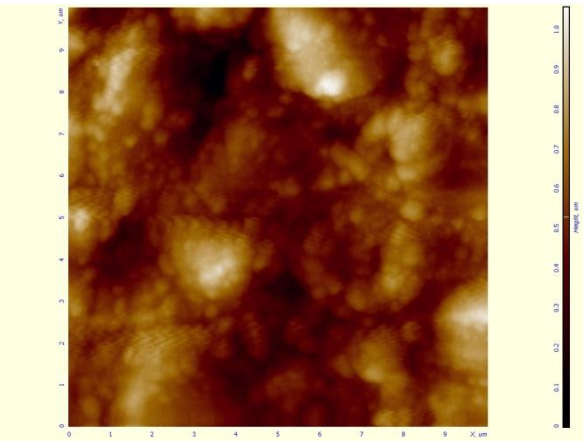

Figure 9. 2D SCM picture (10 x 10μm) on the inside

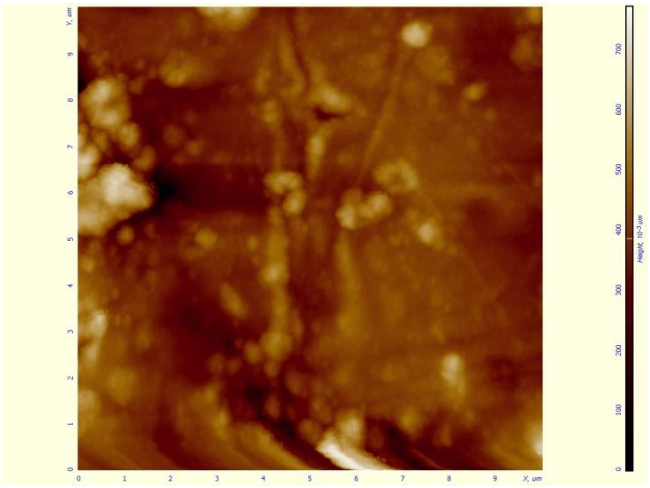

Figure 10. 2D SCM picture (10 x 10µm) on the line.

As can be seen from Fig. 9, the 3D image of Fig.11 confirms that, in the interior, thin layers deposited by sputtering show a higher homogeneity and uniformity, unlike the outer and liner layers (Figs. 12-13) which has an increased roughness, roughness due to the mask that has been applied.

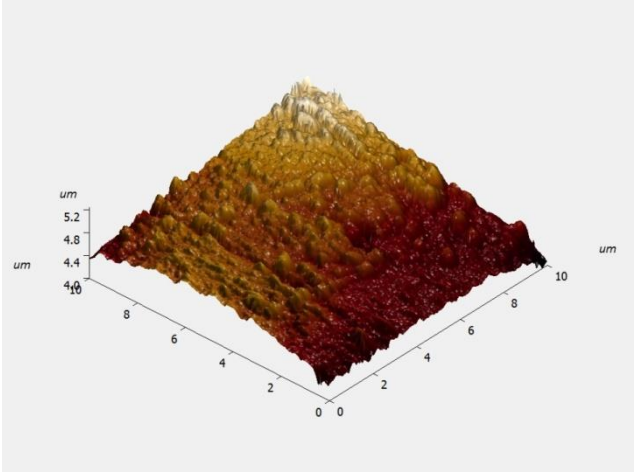

Figure 11. 3D SCM picture (10 x 10µm) on the inside.

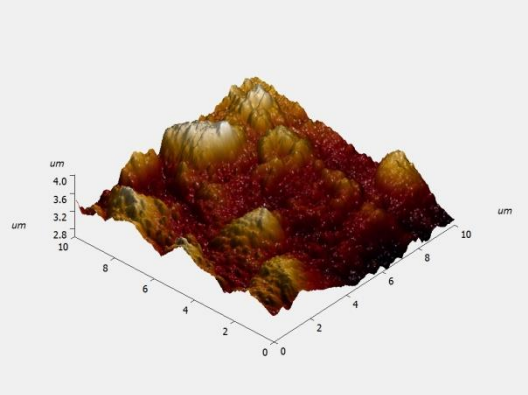

Figure 12. 3D SCM picture (10 x 10µm) on the outside.

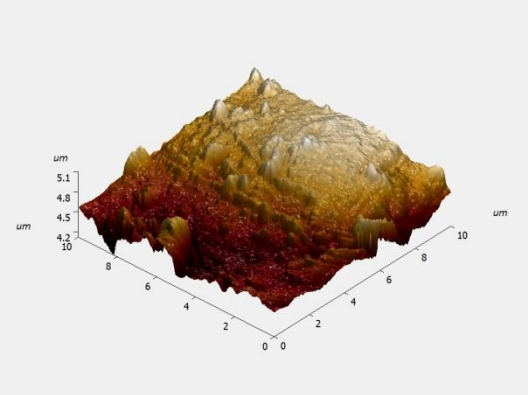

Figure 13. 3D SCM picture (10 x 10µm) on the line.

The PRIMO STAR microscope is capable of investigating samples in transmitted light at a magnification between 4X and 100X. A digital video camera (Axiocam 105) attached to

the microscope is connected to a computer and can enable recording, storage and imaging data in real time [12].

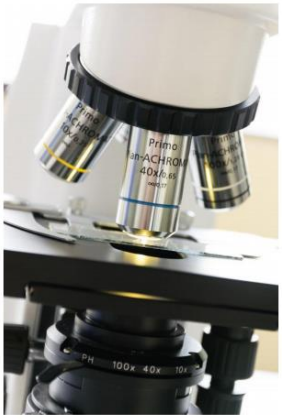

Figure 14. Optical Microscope PRIMO STAR.

The figures below were made with the ZEISS lens microscope at the edge of the magnetic sensor where it is magnified twice, 2.5 times and 4 times respectively. Inside is the upper layer of Cu, the last layer used for the upper contact, and in the outside the initial Cu layer, used for the lower contact.

a) **b)**

Figure 15. Optical images: a) 4.0 x on the deposition limit; b) 2.5 x on the deposition limit.

From the two images obtained with the optical microscope, it can be seen unevenness at the deposition limit; unevenness due to the applied mask, which has not been sufficiently bonded to the substrate or which has not been cut evenly, but this cannot greatly affect the performance of the achieved sensors.

6. PROCESSING OF EXPERIMENTAL RESULTS

As we have shown, the test stand in Fig. 7 is composed of the MF100 AC/DC Magnetic Field Meter, the probe tripod on which we place the sensor and the Y35 ferrite magnet, which is the magnetic field source. We measured the magnetic field in the center of the magnet and at its extremity, from 0.1 cm, 1 cm, 2 cm, 3 cm ... up to 10 cm, this being the distance from the sensor to the Y35 source magnet measured with a graduated ruler.

If we initially position the Ni-Cu sensor in the center of the Y35 magnet, at a distance of 10 cm and then approach the sensor from cm in cm to 0.1 cm, it results in a good linearity in the 1-50 mT range, which can be extended in both directions, if we use other magnetic field sources (Fig. 16).

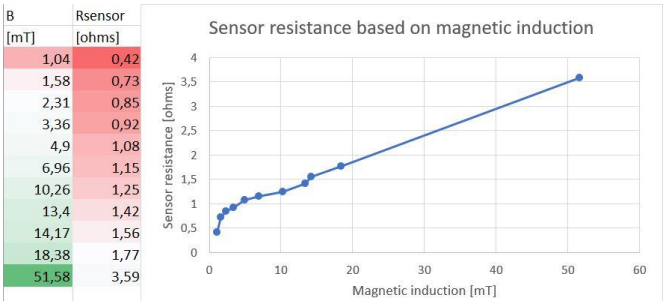

Figure 16. Sensor resistance based on magnetic induction when the sensor is placed in the center of the Y35 magnet.

If we initially position the Ni-Cu sensor at the end of the Y35 magnet, at a distance of 10 cm and then approach the sensor from cm in cm to 0.1 cm, it results in a good linearity in the range of 1 - 100 mT, which can be extended in both directions, if we use other magnetic field sources (Fig. 17).

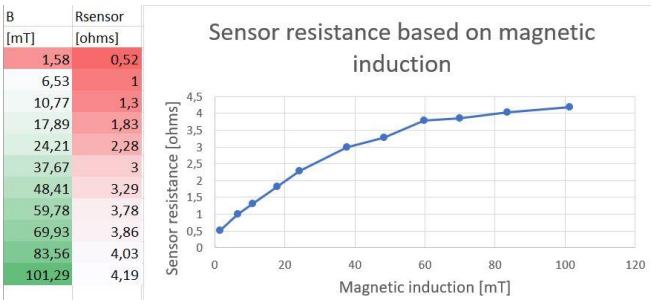

Figure 17. Sensor resistance according to magnetic induction when the sensor is located at the end of the Y35 magnet.

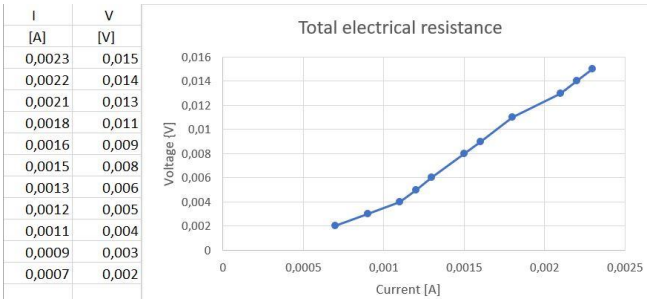

Figure 18 I-V curve of the Ni/Cu sensor.

From this I-V curve results the values of the electrical resistances shown in Fig. 18 for different values of the magnetic field, the measurements being made from 10 cm to 0.1 cm distance from the Y35 magnet. The resistor of the sensor in the graph considers the resistances of the Cu strand conductors and of the Ag contacts, so we have dropped 2.31 Ω of the total resistance (Fig. 19) using the relations below.

It was used 2 stranded wire (15 litz wire) of S = 0.5 mm^2, $\rho_{Cu} = 0.0168x10^{-6}$ Ω m and length l_{Cu} = 0.45 m. Resulted the R_{Cu} = 0.015 Ω from the relations (3) and (4).

$$R = \rho \times l / S \quad (3)$$

$$R_{Cu} = \rho_{Cu} \times l_{Cu} / S_{Cu} = 0.0168x10^{-6}\ \Omega\ m \times 0.45\ m / (0{,}5 \times 10^{-6}\ m^2) = 0.015\ \Omega \quad (4)$$

The contacts were made from Ag conductors with: d = 0.03mm, S_{Ag} = 0.0007 mm^2, $\rho_{Ag} = 1.59 \times 10^{-8}$ Ωm; $l_{Ag} = 5 \times 10^{-2}$ m.

From relation (3) we have for Ag wires:

$$R_{Ag} = \rho_{Ag} \times l_{Ag} / S_{Ag} = 1.59 \times 10^{-8}\ \Omega\ m \times 5x10^{-2}\ m / (0.0007 \cdot 10^{-6}\ m^2) = 1.14\ \Omega \quad (5)$$

Resulted $R_{Ag} = 1.14\ \Omega$ from relation (5).

The contacts between the Ag threads and the sensor were made with the Ag conductive paste at which we considered very small resistances and we did not consider them.

Relation (6) is used for the total resistance and relation (7) is used for the sensor resistance.

$$R_{tot} = 2 \times R_{Cu} + 2 \times R_{Ag} + R_{sensor} \quad (6)$$

$$R_{tot} = 2 \times 0.015 + 2 \times 1.14 + R_{sensor}$$

$$R_{tot} = 2.31 + R_{sensor}$$

$$R_{sensor} = R_{tot} - 2.31 \quad (7)$$

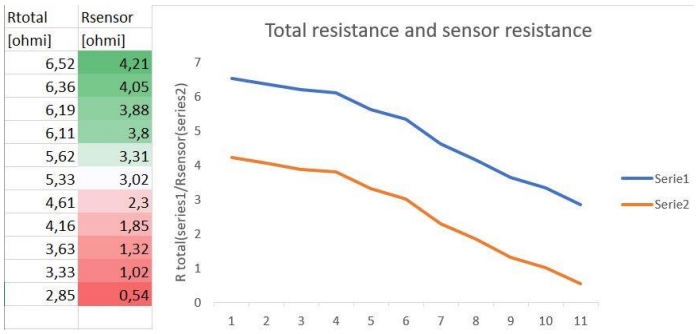

Figure 19. Total resistance and Sensor resistance for the Ni-Cu sensor.

Fig. 19 shows the values for the total resistance and for the sensor resistance, for the magnetic field values, which change with the distance of the Ni-Cu sensor by the Y35 magnet. From the total resistance value, we have dropped 2.31Ω - which represents the value of the resistance of the Cu strands and the resistances of the contacts made from the Ag paste from the relation (7).

This sensor can be used as a magnetic field sensor, at which, in the future, we want to increase the number of thin layers deposited as well as increase the field of measurement of the magnetic field by using other magnetic field sources.

7. CONCLUSIONS

The experiments described in the present paper, ie the deposition of 7 thin layers of Ni-Cu by sputtering and the corresponding measurements, were carried out at the Institute of Multidisciplinary Research for Science and Technology from Valahia University of Targoviste. A total of 26 square and circular shaped sensors were made simultaneously by DC sputtering and the results presented in the paper are those of a sensor in the center of the support layer, 5 mm in diameter and with the sandwich structure (7 layers): SiO_2 (1 mm) / Cu (5 μm) / Ni (12 nm) / Cu (15 nm) /.... Ni (12 nm) / Cu (100 nm); a sensor for which the measurements indicated the best characteristics.

For sensors made, GMR has a low value due to the low number of deposited Ni-Cu layers (7 layers). Although these types of materials are less used in research, we have made the decision to use them because of their high purity (Cu target - 99.99% and Ni target - 99.995%).

Continuity analyzes and edge effects of Ni-Cu thin films were performed with the help of the optical microscope, as well as with the AFM microscope. Measurements were made using the MF100 AC/DC magnetometer, positioning the magnetic sensor with thin Ni-Cu layers, both at the center of the Y35 source magnet ring and outside it. The I-V curve representing the electrical resistance of the Ni-Cu thin-film magnetic sensor located at the end of the Y 35 magnet shows good linearity and sensitivity.

For the measured domain of the magnetic field, the Ni-Cu thin layer magnetic sensor has a good linearity and can be used as a magnetic field sensor. If the sensor has been positioned in the center of the Y 35 ferrite magnet hole, the sensor has a good linearity for a magnetic field between 1 and 50 mT. If the sensor has been positioned at the end of the magnet Y-35 ferrite source, the sensor has a good linearity for a magnetic field of between 1 and 100 mT. In the future, we want to increase the number of magnetic layers deposited to better highlight the GMR and to achieve an extension of the field of magnetic field measurement.

REFERENCES

[1] Nejad, S.N., Fomani, A.A., Mansour, R.R., *IEEE Sensors*, **1**, 387, 2013.
[2] Lenz, J., Edelstein, A.S., *IEEE Sensors Journal*, **6**(3), 631, 2006.
[3] Nejad, S.N., Fomani, A.A., Mansour, R.R., *IEEE Transactions on Magnetics*, **49**(7), 3874, 2013.
[4] Ghosal, S., Kosut, R. L., Ebert, J.L., Porter, L.L., *Proceeding of the 2004 American Control Conference*, **5**, 3930, 2004.
[5] Panina, L., Mohri, K., *Sens. Actuat*., **81**, 71, 2000.
[6] Phan, M., Peng, H., *Progr. Mater Sci*., **53**, 323, 2008.
[7] Ishii, O., Koshimoto, Y., Toshima, T., *IEEE Transactions on Magnetics*, **30** (6), 4611, 2004.
[8] Zhou, Z., Zhou, Y., Chen, L., Lei, C., *Measurement Science and Technology*, **22**(3), 035202, 2011.
[9] Volchkov, S. O., Fernandez, E., Garcia-Arribas, A., Barandiaran, J. M., Lepalovskij, V. N., Kurlyandskaya, G. V., *IEEE Transactions on Magnetics*, **47**(10), 3328, 2011.
[10] Svalov, A.V., Kurlyandskaya, G.V., Hammer, H., Savin, P.A., Tutynina, O.I., *Technical Physics*, **49**(7), 868, 2004.
[11] Antonov, A.S., Iakubov, I.T., *Journal of Physics D: Applied Physics*, **32**, 1204, 1999.
[12] http://www.icstm.ro/ICSTM-equipment.pdf
[13] Cobianu, C., Stan, M.F., Husu, A. G, Fidel, N., *Proceedings of the 13th International Conference on Engineering of Modern Electric Systems*, **1**, 265, 2015.
[14] Cobianu, C., Stan, M.F., Husu, A. G., Fidel, N., *Proceedings of the 9th International Symposium on Advanced Topics in Electrical Engineering*, **1**, 464, 2015.
[15] Panina, L.V., Makhnovsky, D.P., Mapps, D.J., Zarechnyuk, D.S., *Journal of Applied Physics*, **89**, 7221, 2001.
[16] Wang, K., Qiu, Y., Huang, Y., Heard, P., Bending, S., *IEEE Magnetics Conference (INTERMAG*), 1, 2015.
[17] Fernández, E., García-Arribas, A., Barandiarán, J. M., Svalov, A. V., Kurlyandskaya, G. V., Dolabdjian, C. P., *IEEE Sensors Journal*, **15**(11), 6707, 2015.
[18] Ciprian, R., Carbucicchio. M., Palombarini, G., *IEEE Transactions on Magnetics*, **46**(2), 432, 2010.